



ELSEVIER

BASIC SCIENCE

Nanomedicine: Nanotechnology, Biology, and Medicine 6 (2010) 662–671

nanomedicine

www.nanomedjournal.com

Original Article

## In vivo evaluation of the biodistribution and safety of PLGA nanoparticles as drug delivery systems

Boitumelo Semete, PhD<sup>a,\*</sup>, Laetitia Booysen, MSc<sup>a,b</sup>, Yolandy Lemmer, MSc<sup>a,c</sup>,  
Lonji Kalombo, MSc<sup>a</sup>, Lebogang Katata, PhD<sup>a</sup>, Jan Verschoor, PhD<sup>c</sup>, Hulda S. Swai, PhD<sup>d</sup>

<sup>a</sup>Council of Scientific and Industrial Research, Polymers and Bioceramics, Pretoria, South Africa

<sup>b</sup>Department of Pharmacotoxic, North-West University, Potchefstroom Campus, Potchefstroom, South Africa

<sup>c</sup>Department of Biochemistry, University of Pretoria, Pretoria, South Africa

Received 14 August 2009; accepted 28 February 2010

### Abstract

The remarkable physicochemical properties of particles in the nanometer range have been proven to address many challenges in the field of science. However, the possible toxic effects of these particles have raised some concerns. The aim of this article is to evaluate the effects of poly(lactide-co-glycolide) (PLGA) nanoparticles in vitro and in vivo compared to industrial nanoparticles of a similar size range such as zinc oxide, ferrous oxide, and fumed silica. An in vitro cytotoxicity study was conducted to assess the cell viability following exposure to PLGA nanoparticles. Viability was determined by means of a WST assay, wherein cell viability of greater than 75% was observed for both PLGA and amorphous fumed silica particles and ferrous oxide, but was significantly reduced for zinc oxide particles. In vivo toxicity assays were performed via histopathological evaluation, and no specific anatomical pathological changes or tissue damage was observed in the tissues of Balb/C mice. The extent of tissue distribution and retention following oral administration of PLGA particles was analyzed for 7 days. After 7 days, the particles remained detectable in the brain, heart, kidney, liver, lungs, and spleen. The results show that a mean percentage (40.04%) of the particles were localized in the liver, 25.97% in the kidney, and 12.86% in the brain. The lowest percentage was observed in the spleen. Thus, based on these assays, it can be concluded that the toxic effects observed with various industrial nanoparticles will not be observed with particles made of synthetic polymers such as PLGA when applied in the field of nanomedicine. Furthermore, the biodistribution of the particles warrants surface modification of the particles to avoid higher particle localization in the liver.

**From the Clinical Editor:** The aim of this study was to evaluate the effects of poly(lactide-co-glycolide) (PLGA) nanoparticles in vitro and in vivo compared to industrial nanoparticles including zinc oxide, ferrous oxide, and fumed silica. The authors concluded that the toxic effects observed with various industrial nanoparticles is unlikely to be observed with particles made of PLGA. The biodistribution of these particles warrants surface modification to avoid particle accumulation in the liver.

© 2010 Elsevier Inc. All rights reserved.

**Key words:** Nanoparticles; Nanomedicine; PLGA; Biodistribution; Toxicity

Nanotechnology has become one of the critical research endeavors of the 21st century; thus, researchers must intensify their efforts to further understand the potential effects of these materials on biological systems. Materials on a nanometer scale have unique physicochemical properties that are due to their small size, surface area, chemical composition, surface structure, solubility, and shape<sup>1</sup>; these properties have thus far been

utilized in various fields including drug and gene delivery, imaging, and diagnostics.<sup>2–4</sup>

Much work in elucidating the possible effects of nanomaterial has been conducted on metal nanoparticles. This is primarily due to the rapid increase in the production of these materials, fueled by the growing need for the properties that these materials provide. Particle toxicity has been studied over a fair number of years, particularly in lung injury in the case of metal nanoparticles, ambient ultrafine particles, asbestos fibers, and dust particles.<sup>3,5</sup> Various reports have indicated that these particles induce oxidative injury, inflammation, fibrosis, and cytotoxicity.<sup>3,6,7</sup> It has been reported that smaller particles (aerodynamic diameter <100 nm) have a greater propensity to lead to pulmonary toxicity owing to their small size, larger

No conflict of interest was reported by the authors of this paper.

\*Corresponding author. Council for Scientific and Industrial Research, Polymers and Bioceramics, P.O. Box 395, Pretoria 0001, South Africa.

E-mail address: Bsemete@csir.co.za (B. Semete).

1549-9634/\$ – see front matter © 2010 Elsevier Inc. All rights reserved.  
doi:10.1016/j.nano.2010.02.002

Please cite this article as: B. Semete, et al. In vivo evaluation of the biodistribution and safety of PLGA nanoparticles as drug delivery systems. *Nanomedicine: NBM* 2010;6:662–671, doi:10.1016/j.nano.2010.02.002

surface area, and deeper penetration into the lungs than bulkier particles of the same material.<sup>3</sup>

However, with regard to nanomedicine, the adverse effects of the particles have not been extensively studied, possibly because in nanomedicine, mainly biodegradable, biocompatible, and U.S. Food and Drug Administration–approved materials are used.<sup>2,8</sup> However, concerns over the effects of the physicochemical properties of nanoparticles such as size, surface area, and molecular weight of the material warrants further investigation.

It has been speculated that the specific surface area of nanoparticles is responsible for the potential adverse effects that nanoparticles could have in drug delivery applications.<sup>3</sup> This is because smaller particle size increases the specific surface area, thus exposing more atoms or molecules (and thus more reactive groups of the material) on the surface to molecules that would not have access to larger particles.<sup>9</sup> This aspect could form the basis of the production of reactive oxygen species, wherein the electron donor or acceptor sites on the nanomaterial interact with molecular oxygen, resulting in the formation of superoxide anion or hydrogen peroxide, which subsequently oxidize other chemical species by an electron transfer mechanism. The production of reactive oxygen species has been reported as the most likely mechanism by which these particles exert a toxic effect.<sup>3</sup> Therefore, the specific surface area is an important parameter to consider when elucidating the possible adverse effects of a nanomaterial. For efficient drug delivery, the nanosize range of particles is the “holy grail”, because it can facilitate increased intracellular uptake of the drugs to specific cellular targets—a process that is not very efficient in conventional formulations. This, in turn, improves the bioavailability of therapeutic compounds.<sup>4,10</sup> As suggested by various studies on ultrafine particles,<sup>5,7</sup> this beneficial property of nanoparticles’ ability to be taken up intracellularly could also be a source of concern, given that the nanosize range of the particles enables unique interaction with biological materials such as key proteins in the cellular pathways, which could possibly culminate in adverse effects.<sup>6</sup>

With the above-mentioned uncertainties about the potential effects of specific surface area, size, and composition of polymeric nanoparticles in mind, our team focused on elucidating the effect of poly(lactide-co-glycolide) (PLGA) nanoparticles, as well as particles composed of ferrous oxide (Fe<sub>2</sub>O<sub>3</sub>), zinc oxide (ZnO), and fumed silica (SiO<sub>2</sub>) on cell viability. Also studied was the effect of PLGA nanoparticles and ZnO particles on various tissues after oral administration. Various reports have indicated that the oral route of drug delivery is still the preferred route and will dominate the drug delivery market for decades to come.<sup>11</sup> Hence, for the purpose of the study we explored the effect of these particles when administered orally to Balb/C mice.

In addition, the nanosize range of nanoparticles has been reported to facilitate the crossing of various biological barriers such as the blood-brain barrier (BBB), the skin, and the tight junctions of various epithelial layers.<sup>12</sup> Thus, we further explored the tissue distribution of PLGA particles after oral administration to determine to which tissues these particles localize.

## Methods

### Preparation of PLGA particles

Nanoparticles were prepared with poly(dl-lactide-co-glycolide) (PLG) 50:50 (molecular weight 45,000–75,000) (Sigma-Aldrich, Johannesburg, South Africa) using a modified double-emulsion solvent evaporation technique.<sup>13</sup> Aqueous phosphate-buffered saline pH 7.4 was emulsified for a short period with a solution of 100 mg PLGA dissolved in 8 mL of ethyl acetate (EA), by means of a high-speed homogenizer (Silverson L4R, Silverson Machines Limited, Buckinghamshire, United Kingdom) with a speed varying between 3000 and 5000 rpm. The resulting water-in-oil (w/o) emulsion was transferred into a specific volume of an aqueous solution of 1% (wt/vol) polyvinyl alcohol (molecular weight 13,000–23,000 and partially hydrolyzed: 87–89%) used as an emulsion stabilizer, also purchased from Sigma-Aldrich. The mixture was further emulsified for 5 minutes by homogenization at 8000 rpm. The double emulsion (w/o/w) obtained was directly fed into a benchtop Buchi minispray dryer (Model B-290, BÜCHI Labortechnik AG, Flawil, Switzerland) and spray-dried at a temperature ranging between 95° and 110°C, with an atomizing pressure varying between 5 and 8 bars.

To prepare fluorescently labeled PLGA nanoparticles, Rhodamine-6G (Sigma-Aldrich) was dissolved in 2.5 mL EA (0.5 mg/mL), which was added to the solution of PLGA in EA. In cases wherein the particles were labeled with coumarin (Sigma-Aldrich), it was also dissolved in 2.5 mL EA at 0.5 mg/mL. For the preparation of these fluorescently labeled particles, the w/o/w emulsion was left overnight to allow evaporation of the solvent. The pellet recovered after centrifugation was then lyophilized using the Virtis Benchtop freeze dryer (SP Industries, Gardiner, New York). Spray-drying was also applied. The results presented in this article are from the spray-dried formulation, because this method proved to be easier to scale up for the application of these nanoparticles.

### Particle size, zeta potential, and surface morphology

Particle size and size distribution were measured by dynamic laser scattering or photon correlation spectroscopy using a Malvern Zetasizer Nano ZS (Malvern Instruments, Worcester-shire, United Kingdom). For each sample, 1–3 mg of nanoparticles were suspended in distilled water, then vortexed and/or sonicated for a few minutes. Each sample was measured in triplicate. The zeta potential was also determined using the same instrument, in pH 6.8. The morphology of PLGA nanoparticles was analyzed using a scanning electron microscope (LEO 1525 Field Emission scanning electron microscope, Zeiss, Oberkochen, Germany).

### Surface area determination

Surface area measurements were carried out according to the conventional BET method,<sup>14</sup> using the Nova 1000e surface area and pore size analyzer (Quantachrome Instruments, Boynton Beach, Florida). The method is based on isothermal adsorption of nitrogen onto the particles at liquid nitrogen temperature and relative pressures (P/P<sub>0</sub>) ranging from 0.05 to 0.2. Spray-dried



PLGA particles (50 mg), Fe<sub>2</sub>O<sub>3</sub>, and SiO<sub>2</sub> (obtained from Walter Focke, University of Pretoria, Department of Chemical Engineering) were degassed by heating under vacuum and used for the measurement. The adsorbed nitrogen volume at 77.3 K was calculated by measuring the pressure change resulting from the adsorption of nitrogen gas onto the surface of particles. The area per molecule value for nitrogen was taken at 162 nm<sup>2</sup>, and using this value, the total surface area of the sample was determined. The specific surface area was calculated by dividing the surface area by the sample weight.

#### *In vitro cell viability assay*

Caco-2 cells (human colorectal carcinoma) and HeLa (human epithelial carcinoma) cells were purchased from Highveld Biologicals, Johannesburg, South Africa. The cells were cultured in 25-mL flasks at 37°C in humidified atmosphere (90% humidity), 5% CO<sub>2</sub>, Dulbecco's minimal essential medium, 1% (wt/vol) nonessential amino acids, 1% (wt/vol) glutamine, 10% (vol/vol) fetal bovine serum, penicillin, (100 U/mL), and streptomycin (100 µg/mL). Stocks of the cells were prepared in culture medium containing 80% (vol/vol) fetal bovine serum and 10% (vol/vol) dimethyl sulfoxide and kept in liquid nitrogen until further use. The cells were maintained according to routine cell culture procedures. To determine cell viability after exposure of all cell lines to different concentrations of PLGA nanoparticles of an average size of 374 nm incubated for 24 hours, the WST assay (Quick Cell Proliferation Assay Kit II, Mountain view, California) was performed according to manufacturer's instructions. This colorimetric cell proliferation kit allows for easy and reliable colorimetric determination of viable cell numbers with excellent sensitivity and linearity. The kit utilizes the tetrazolium salt WST-1, which is reduced to water-soluble orange formazan by cellular mitochondrial dehydrogenase present in viable cells. The amount of formazan dye, determined by the absorbance at 450 nm with a reference wavelength at 630 nm, is directly proportional to the number of living cells. Fe<sub>2</sub>O<sub>3</sub>, SiO<sub>2</sub>, and ZnO (Sigma) nanoparticles were used as controls.

#### *In vivo studies*

##### *Animals*

Unchallenged Balb/C female mice weighing between 20 and 25 g were selected and housed under standard-environment conditions at ambient temperature of 25°C. Animals were humanely cared for and supplied with food and water ad libitum. Ethics approval was obtained for this study from the Ethics Committee for Research on Animals (ECRA), Tygerberg, Cape Town, South Africa.

##### *Histopathology assays*

Mice were placed into different groups with three mice per group based on the particles they were treated with and the time frame of treatment. The different groups consisted of animals treated separately with 4 mg PLGA particles, 4 mg SiO<sub>2</sub>, and 4 mg ZnO nanopowder (purity >99%; Sigma-Aldrich) by mouth. The latter was used as a positive control in this study, as it is known to have toxic effects on tissues.<sup>15</sup> Polystyrene beads (Sigma-Aldrich, 300 nm) were used as negative control. Group 1

was treated for 24 hours, group 2 was treated daily for 5 days, and group 3 was treated daily for 10 days. Mice were euthanized on day 1, 5 and 7 respectively. The study was repeated once, except that the second time mice were overdosed with the particles (i.e., 60 mg of PLGA particles and 60 mg of SiO<sub>2</sub> and polystyrene beads for 24 hours, for 5 days, and for 10 days. Full necropsies were conducted on the mice following humane euthanasia. The brain, heart, kidney, liver, lung, spleen, gonad (female genitalia), large and small intestines, pancreas, stomach, and thymus were collected from each animal. Tissues were fixed with formalin, and tissue sections cut and processed using routine histological methods in an automated system. Sections of 5 µm were prepared after paraffin embedding. The slides obtained were stained with routine hematoxylin and eosin staining method in an automated stainer.

#### *Tissue distribution assays of PLGA nanoparticles*

To determine the biodistribution of the nanoparticles, fluorescently labeled particles were orally administered to mice. The mice were grouped with three mice per group, and the study was repeated three times. Group 1 was treated with 4 mg of rhodamine-PLGA nanoparticles in 0.2 mL sterile saline by oral gavage. Group 2 was treated with 4 mg coumarin-labeled PLGA nanoparticles in 0.2 mL sterile saline by oral gavage. The two fluorescent dyes were used to determine if there any differential biodistribution occurred based on the fluorescent dyes. Furthermore, rhodamine and coumarin were spray-dried without encapsulating into PLGA nanoparticles and orally administered to mice.

In addition, 4 mg of fluorescently labeled polystyrene beads were orally administered as a control to group 3. The mice were killed via cervical dislocation. The brain, heart, kidneys, liver, lungs, and spleen as well as plasma were collected. The tissues were homogenized on ice in 2 mL phosphate-buffered saline, and diluted 100 times. The resulting diluted homogenates were analyzed for fluorescent particles on the FLx8000 Biotek plate reader (Biotek, Winooski, Vermont) at excitation and emission wavelengths of 488 nm and 525 nm, respectively. The tissues were further analyzed via confocal microscopy to determine if the fluorescence observed was still in the particulate matter or had been leached out.

## **Results**

#### *Particle size, zeta potential, surface morphology, and specific surface area*

Various parameters were optimized to obtain an average particle size ranging between 200 and 350 nm, with an average polydispersity index of 0.1 observed when freeze-drying was used (Figure 1, A). However, the polydispersity index of the spray-dried formulation was higher (0.2 as observed in Figure 1, B) with a size range of 300 nm to 1 µm. The particles had a zeta potential between -10 and -18 mV. The spray-dried particles were characterized by a very smooth surface, similar to the freeze-dried particles as depicted by scanning electron microscopy (images in Figure 1, A and B). However, the

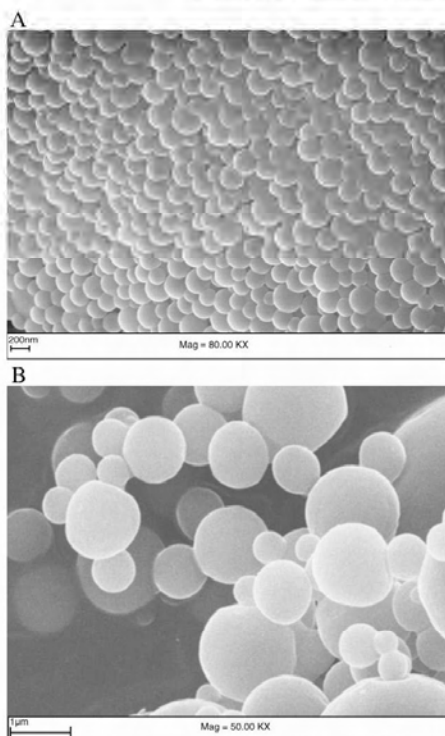


Figure 1. (A) SEM picture of freeze-dried formulation (prepared with 40 mL 1% wt/vol polyvinyl alcohol). Bar = 200 nm. (B) Spray-dried formulation with the same parameters. Bar = 1 μm.

particles were not equivalent in size. The freeze-dried PLGA nanoparticles had a specific surface area ranging between 3 and 10 m<sup>2</sup>/g, whereas a specific surface area ranging between 15 and 25 m<sup>2</sup>/g was found for ZnO nanoparticles at a size of 50–150 nm. Fe<sub>2</sub>O<sub>3</sub> and SiO<sub>2</sub> had specific surface areas of 11–15 m<sup>2</sup>/g and 755–1043 m<sup>2</sup>/g, respectively, and a size range of 100–250 nm. The *in vitro* and *in vivo* data presented in the manuscript are for the freeze-dried PLGA particles.

#### *In vitro* cell viability assays

The *in vitro* cytotoxicity of PLGA nanoparticles, SiO<sub>2</sub>, Fe<sub>2</sub>O<sub>3</sub> particles, and ZnO particles was determined at concentrations of 0.1, 0.01 and 0.001 mg/mL, on Caco-2 cells and Hela cells via the WST assay. The results depicted in Figure 2 indicate that, compared with untreated cells (control), the Hela and Caco-2 cell lines retained more than 75% viability when treated with various concentrations of PLGA nanoparticles, SiO<sub>2</sub>, and Fe<sub>2</sub>O<sub>3</sub>. This result supports literature indicating that amorphous silica, as was used in this study, is not toxic to cells.<sup>15</sup> However, ZnO

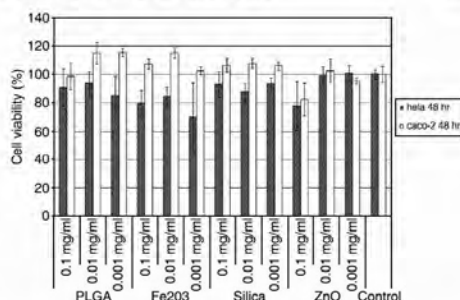


Figure 2. Effects of poly(lactide-co-glycolide), ferrous oxide, and fumed silica particles on percentage viability of Caco-2 and Hela cell lines as shown by a WST assay. The data are representative of two repeats of n = 6; error bars indicate SEM.

nanopowder resulted in a significant reduction in cell viability, as indicated in Figure 2. This result is also in accordance with those of Sharma et al 2009, where it was indicated that ZnO nanoparticles are toxic to cells.

#### *Histopathology* assays

Subsequent to oral administration of PLGA particles as well as polystyrene beads for 1, 5, and 10 days, no pathological lesions were detected in the respective groups that could be suggestive of toxicity. (Images of the polystyrene-treated group are not included, as they are similar to those of PLGA particles.) The data were in accordance with those of the saline control group. None of the analyzed tissues exhibited any lesions, even at 60 mg PLGA, as depicted in Table 1. The group treated with amorphous SiO<sub>2</sub> particles showed no noticeable lesion (images not included). The group of mice that were treated with 4 mg ZnO for 24 hours died, and a subset of the mice showed weight loss. Based on these observations, the positive control was not continued for the 5- and 10-day studies. Thus, it can be suggested from these data that PLGA particles at the various concentrations administered do not exhibit any toxicity in mice based on histopathological assays.

#### *Tissue distribution* assays

The fluorescently labeled particles were initially not detected in the 5-μm tissue sections via fluorescent microscopy, as a result of the intense autofluorescence of the tissues. Thus, a fluorometer was used to detect fluorescence in the tissue homogenates. The data were normalized with the negative control, which was tissue from mice treated with only saline. The background fluorescence from these tissues was subtracted from the experimental tissue fluorescence readings to exclude the effect of autofluorescence. The percentage particles detected was expressed as the ratio of the fluorescence unit of each tissue relative to the sum of fluorescence units of all tissues analyzed and graphically illustrated in Figure 3 and listed in Table 2 for each tissue. From these data it is evident that most of the particles were detected in the liver at 40.04% ± 8.42%, followed by the



**Table 1**  
 Histopathology and confocal images of different mouse tissues after oral administration of fluorescently labeled PLGA or fumed silica

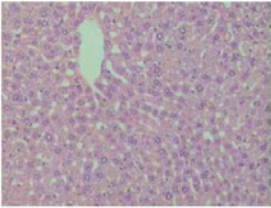
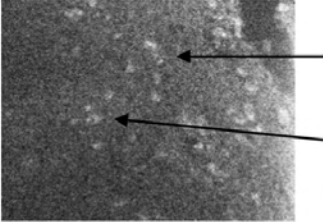
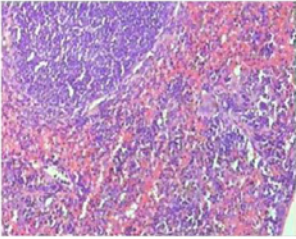
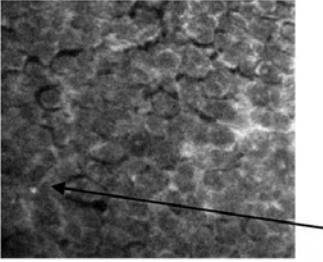
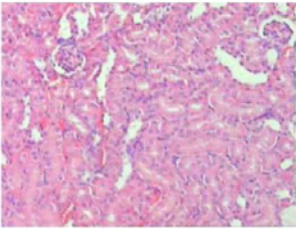
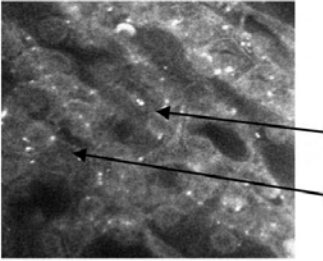
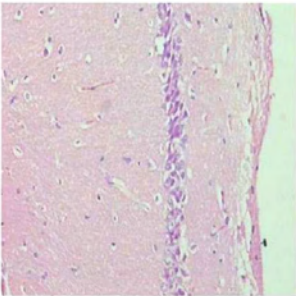
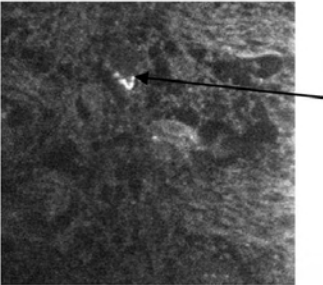
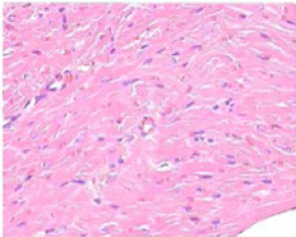
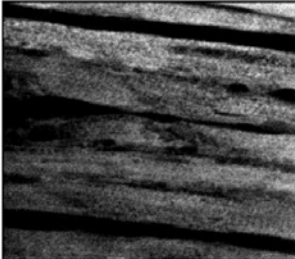
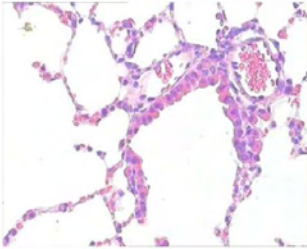
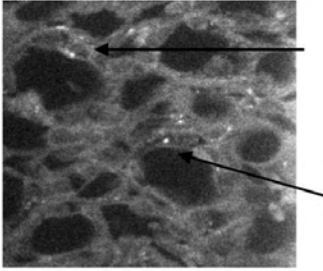
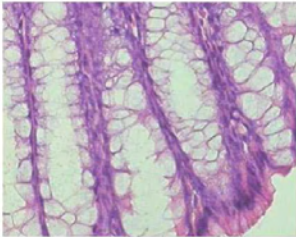
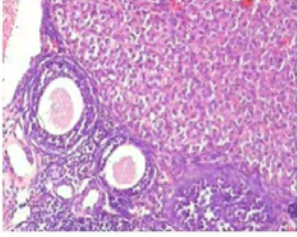
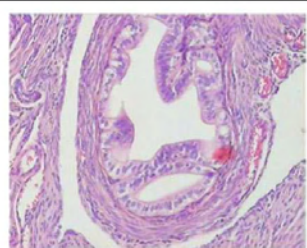
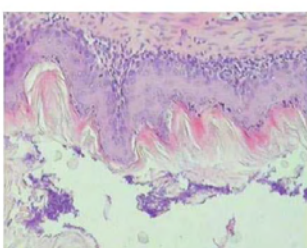
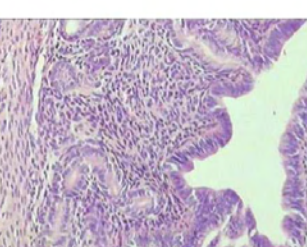
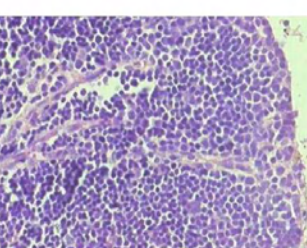
Tissue	Tissues treated with PLGA nanoparticles (fumed SiO <sub>2</sub> gave results similar to the PLGA particles)	Confocal microscope images (62× magnification) of tissue sections, 1 day after administration of rhodamine-labeled particles
Liver		
Spleen red pulp		
Kidney		
Hippocampus in the cerebrum		

Table 1 (continued)

Tissue	Tissues treated with PLGA nanoparticles (fumed SiO <sub>2</sub> gave results similar to the PLGA particles)	Confocal microscope images (62× magnification) of tissue sections, 1 day after administration of rhodamine-labeled particles
myocardium		
Terminal bronchiolus and lung		
Large intestines		Not analyzed via confocal microscope
Ovarian follicles and corpus luteum		Not analyzed via confocal microscope

(continued on next page)

Table 1 (continued)

Tissue	Tissues treated with PLGA nanoparticles (fumed SiO <sub>2</sub> gave results similar to the PLGA particles)	Confocal microscope images (62× magnification) of tissue sections, 1 day after administration of rhodamine-labeled particles
Fallopian duct		Not analyzed via confocal microscope
Glandular gastric mucosa		Not analyzed via confocal microscope
Endometrium of uterine mucosa		Not analyzed via confocal microscope
Thymus lymphoid tissues		Not analyzed via confocal microscope

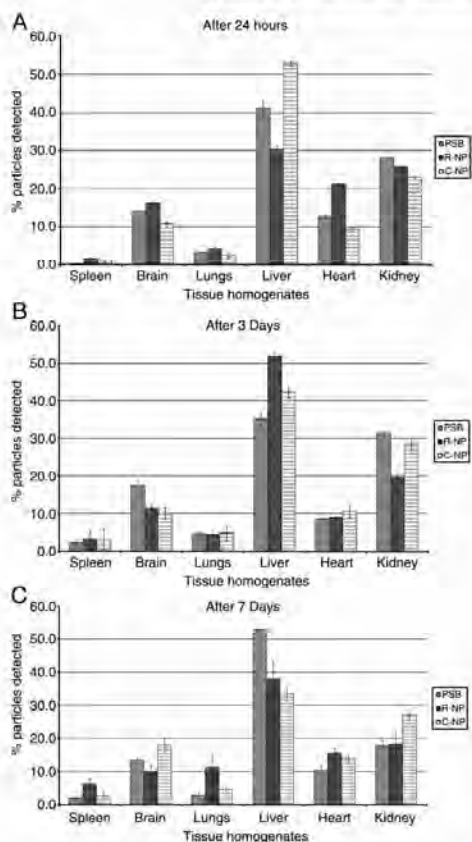


Figure 3. Tissue distribution graphically represented as a measure of percentage of particles detected of the total particles. The data represent three repeats of  $n = 6$ ; error bars indicate SEM. (A) 24 hours, (B) 3 days, (C) 7 days. PSB, polystyrene beads; R-NP, rhodamine nanoparticles; C-NP, coumarin nanoparticles.

kidney ( $25.97\% \pm 7.09\%$ ), heart ( $11.92\% \pm 3.16\%$ ), and brain ( $12.86\% \pm 2.82\%$ ) throughout all 7 days in which the tissues were analyzed. Plasma was also analyzed from day 3 as indicated in Figure 4, but only very small amounts of the particles were detected. Confocal images of the tissues after 1 day of administration of the rhodamine-labeled particles are presented in Table 1, where we have shown, using unstained tissues for comparison, that the fluorescent particles can be detected within the various tissues. It has been reported that rhodamine release from nanoparticles is very slow, and therefore, the detection of fluorescence in the different tissues can be considered to be that of the rhodamine associated with the PLGA nanoparticles.<sup>16,17</sup> It must be emphasized that the confocal images do not correlate to

Table 2

Percentage particles detected, calculated as a function of total particles

Organ	% Particles detected								
	1 day			3 days			7 days		
	PSB	R-NP	C-NP	PSB	R-NP	C-NP	PSB	R-NP	C-NP
Brain	14.3	16.4	10.8	17.6	11.5	10.2	13.6	10.1	18.1
Heart	12.8	21.3	9.4	8.7	9.1	10.7	10.5	15.7	14
Kidney	28.2	25.9	23.1	31.5	19.7	28.6	18	18.3	27.1
Lung	3.4	4.2	2.7	4.8	4.5	4.9	2.9	11.4	4.7
Liver	41.3	30.5	52.9	35.2	51.9	42.4	55	38.1	33.4
Spleen	0.2	1.7	1.1	2.3	3.3	3.3	2	6.4	2.7

PSB, polystyrene beads; R-NP, rhodamine nanoparticles; C-NP, coumarin nanoparticles.

Data are expressed as a representation of percentage particles detected of total particles;  $n = 6$ .

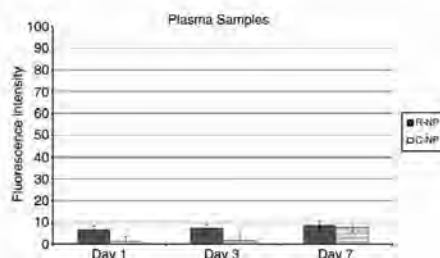


Figure 4. Fluorescence detection in plasma represented as a function of fluorescence intensity. R-NP, rhodamine nanoparticles; C-NP, coumarin nanoparticles.

the quantity of the particles in the tissues, but only indicate the presence of the particles in the respective tissues and also indicate the particulate nature of the fluorescence, suggesting that the observed fluorescence is that of rhodamine in the nanoparticles and not leached rhodamine.

### Discussion

The toxicity of nanoparticles involves physiological, physicochemical, and molecular considerations. Extensive studies on industrial nanoparticles investigating these parameters have been conducted, but not much is known about nanoparticles that are used for therapeutic purposes. At present, PLGA is used extensively for drug delivery applications.<sup>4,18</sup> It is with this in mind that this study focused on elucidating the effect of PLGA nanoparticles in vitro and in vivo. Much controversy still exists regarding the potential adverse effects, so there is a need for reports indicating the safety of these materials. The particles analyzed had specific surface areas within a similar range, except for the amorphous silica, which had a higher specific surface area. Thus, although these PLGA particles had a surface area similar to that of ZnO, which served as a positive control, no toxic effect as presented in the viability



Table 3  
Fluorescence units of tissues after oral administration of fluorescently labelled particles or spray dried fluorophores

	Brain	Heart	Kidney	Liver	Lungs	Spleen
RH-NPs day 1	35.9	47.8	53.9	67.1	8.9	3.8
RH day 1	2.5	1	11.8	4	1	1
RH-NPs day 3	36.3	28.4	170.4	63.4	14.4	10.5
RH day 3	4.8	1	4.2	6	1	1
RH NPs day 7	40.3	64.8	156.8	93.2	43.2	29.5
RH day 7	5	1	2	2	1	1
C-NPs day 1	35.4	31.4	75.6	176.3	8.4	3.5
C day 1	1.3	1	4.8	1	14.3	1
C-NPs day 3	50.7	54	171	214.3	27.7	24
C day 3	1	1	5.8	50.3	10.1	1
C-NPs day 7	66.9	53	110.9	140.7	18.9	9.9
C day 7	−0.2	1	8.8	73.3	1	1

RH, Rhodamine; NPs, nanoparticles, C, Coumarin. n = 3.

assays was observed. This suggests that the biodegradability and biocompatibility of PLGA nanoparticles facilitates their safe use in medical applications.

In vitro cytotoxicity of the respective particles was tested in two different cell lines. The PLGA nanoparticles were shown to have no cytotoxic effects on the cells. Although specific surface area has been reported to be causal in some of the observed toxicities in metal nanoparticles,<sup>6</sup> it is clear from the viability assay that the surface area of PLGA particles did not significantly affect the viability of the cells analyzed. Second, it can be suggested that the chemical composition of the PLGA nanoparticles did not contribute to toxicity. As polyesters in nature, PLGA undergoes hydrolysis and enzymatic degradation upon implantation into the body, forming biologically compatible moieties that can be metabolized (lactic acid and glycolic acid) and are eventually removed from the body by the citric acid cycle.<sup>19</sup> These PLGA biodegradation products are formed at a very slow rate and hence do not affect normal cell function. Although SiO<sub>2</sub> nanopowder and Fe<sub>2</sub>O<sub>3</sub> particles had larger specific surface areas as compared with PLGA particles, they did not exhibit any toxicity, thus supporting the observation that surface area is not the main determinant of toxicity in nanoparticulate structures.

Subsequent to oral administration of polystyrene beads, rhodamine-labeled PLGA particles, as well as coumarin-labeled PLGA particles in the respective groups, particles were detected in all tissues evaluated. The highest percentage of particles was detected in the liver, followed by the kidney, the brain, and the heart, as shown in Table 2. To confirm that the fluorescence detected is from the encapsulated fluorophores, Table 3 illustrates the fluorescence measured of the encapsulated fluorophores versus the unencapsulated but spray-dried fluorophores. Thus, from these data it is evident that rhodamine and coumarin are cleared from the tissues within 1 day, and thus low concentrations are detected in comparison with when these fluorophores are encapsulated in PLGA nanoparticles. This result also confirms that these nanoparticles are able to cross cellular barriers such as the BBB and reach hard-to-target tissues—in accordance with work published elsewhere.<sup>12,20</sup> However, we have also shown that although these particles are detected in various tissues within a 7-day period, these particles do not cause any morphological

pathology in the respective tissues even at high doses (i.e., 60 mg per 25g mice). As demonstrated by the histopathology assays conducted, no lesions or inflammation was observed in the brain. The lowest concentrations were observed in the spleen and lungs. This result could indicate that for oral administration of PLGA particles for drug delivery purposes, these particles will have to be surface-modified with hydrophilic molecules such as polyethylene glycol to minimize opsonization of the particles, thus increasing the circulation time in the blood with the eventual effect of minimizing the amount of particles that reach the liver. Thus far, various hydrophilic surfactants have been used to minimize opsonization.<sup>21</sup> Poloxamers, poloxamines, and other polymers such as chitosan can also be used for this purpose.<sup>22</sup> This will, in turn, minimize first-pass metabolism of the encapsulated drugs. Various groups have also reported modification of the particles with peptides or proteins.<sup>16</sup>

Drug delivery systems such as PLGA nanoparticles will provide an ideal carrier system to various tissues that are generally hard to target even with oral administration, as presented in this study as well as other studies.<sup>18,20</sup> Because of its ability to cross the BBB, this system will present a means of effectively treating neurological and psychiatric disorders,<sup>16</sup> as well as other disseminated diseases such as tuberculosis, by administering the nanoencapsulated drugs orally or via any other noninvasive modes. Furthermore, according to this study, PLGA nanoparticles are safe to use as a drug delivery system, although many concerns still exist regarding the safety of nanomaterials in general.

From this study conducted with biodegradable and biocompatible PLGA nanoparticles, it is clear that these particles are not toxic in cell culture and when orally administered at the mentioned doses to Balb/c mice. More studies need to be conducted with other polymeric nanoscale drug delivery systems, to evaluate their safety. It is clear from the biodistribution data that nanoscale drug delivery systems will be suitable to improve the permeability, and thus the bioavailability of therapeutic compounds. With this approach, delivery of drugs that have poor permeability and solubility can be greatly enhanced with safe and effective drug delivery systems.

#### Acknowledgments

We thank Kobus Venter at the Medical Research Council for assisting with the mice studies, Robyn Brackin at the Council of Scientific and Industrial Research for assistance with the confocal images, and Dr. Willem Botha of Vetpath Laboratories for assisting with the histopathology assays.

#### References

- Magenheim B, Benita S. Nanoparticle characterization: a comprehensive physicochemical approach. *S T P Pharm Sci* 1991;1:221–41.
- Duncan R. Nanomedicine gets clinical. *Materials Today* 2005;8:16–7.
- Nel A, Xia T, Madler L, Li N. Toxic potential of materials at the nanolevel. *Science* 2006;311:622–7.
- Panyam J, Labhasetwar V. Biodegradable nanoparticles for drug and gene delivery to cells and tissue. *Adv Drug Deliv Rev* 2003;55:329–47.
- Stone V, Donaldson K. Nanotoxicology: signs of stress. *Nat Nanotechnol* 2006;1:23–4.

6. Li N, Xia T, Nel AE. The role of oxidative stress in ambient particulate matter-induced lung diseases and its implications in the toxicity of engineered nanoparticles. *Free Radic Biol Med* 2008;44:1689–99.
7. Oberdorster G, Maynard A, Donaldson K, Castranova V, Fitzpatrick J, Ausman K, et al. Principles for characterizing the potential human health effects from exposure to nanomaterials: elements of a screening strategy. *Particle Fibre Toxicol* 2005;2:8–43.
8. McNeil SE. Nanotechnology for the biologist. *J Leukocyte Biol* 2005;78:585–94.
9. Liveridge GG, Cundy KC. Particle size reduction for improvement of oral bioavailability of hydrophobic drugs: I. Absolute oral bioavailability of nanocrystalline dexamethasone in beagle dogs. *Int J Pharm* 1995;125:91–7.
10. Desai MP, Labhasetwar V, Amidon GL, Levy RJ. Gastrointestinal uptake of biodegradable microparticles: effect of particle size. *Pharm Res* 1996;13:1838–45.
11. Wilkinson JM. Roadmapping medical devices. *Medical Device Link* 2006;6:1-0090 Ref Type: Electronic Citation. Available at: <http://www.devicelink.com/mdt/archive/06/06/014.html>.
12. Koziara JM, Lockman PR, Allen DD, Mumper RJ. In situ blood brain barrier transport of nanoparticles. *Pharm Res* 2003;20:1772–8.
13. Lamprecht A, Ubrich N, Hombreiro Perez M, Lehr CM, Hoffman M, Maincent P. Biodegradable monodispersed nanoparticles prepared by pressure homogenization-emulsification. *Int J Pharm* 1999;184:97–105.
14. Brunauer S, Emmett PH, Teller E. Adsorption of gases in multimolecular layers. *J Am Chem Soc* 1938;60:309–19.
15. Merget R, Bauer T, Klüpper H, Philippou S, Bauer H, Breitzstadt R, et al. Health hazards due to the inhalation of amorphous silica. *Arch Toxicol* 2002;75:625–34.
16. Vergoni AV, Tosi G, Tacchi R, Vandelli MA, Bertolini A, Costantino L. Nanoparticles as drug delivery agents specific for CNS: in vivo biodistribution. *Nanomed Nanotechnol Biol Med* 2009;5:369–77.
17. Tosi G, Costantino L, Rivasi F, Ruozi B, Leo E, Vergoni AV, et al. Targeting the central nervous system: in vivo experiments with peptide-derivatized nanoparticles loaded with Loperamide and Rhodamine-123. *J Control Release* 2007;122:1–9.
18. Jais RA. The manufacturing techniques of various drug loaded biodegradable poly(lactide-co-glycolide) (PLGA) devices. *Biomaterials* 2000;21:2475–90.
19. Campbell MK. *Biochemistry*. Philadelphia: Saunders College Publishing; 1995. p. 365–84.
20. Lockman PR, Mumper RJ, Khan A, Allen DD. Nanoparticle technology for drug delivery across the blood-brain barrier. *Drug Dev Ind Pharm* 2002;28:1–13.
21. Storm G, Belliot SO, Daemen T, Lasic DD. Surface modification of nanoparticles to oppose uptake by the mononuclear phagocyte system. *Adv Drug Deliv Rev* 1995;17:31–48.
22. Torchilin VP, Tribetskoy VS. Which polymers can make nanoparticulate drug carriers long-circulating? *Adv Drug Deliv Rev* 1995;16:141–55.